Chinese Chemical Letters 35 (2024) 108723

Contents lists available at ScienceDirect

Chinese Chemical Letters

journal homepage: www.elsevier.com/locate/cclet

Photocatalytic transformation of selected biomass derivatives to value added chemicals and hydrogen fuel

Xiangjun Liu, Shuai Zhang, Miao Wang, Junqi Wang*

School of Human Settlements and Civil Engineering, Xi'an Jiaotong University, Xi'an 710049, China

ARTICLE INFO

Article history:
Received 3 March 2023
Revised 6 June 2023
Accepted 23 June 2023
Available online 24 June 2023

Keywords:
Photocatalytic transformation
Biomass
Semiconductor material
H_2
High value-added chemical

ABSTRACT

Biomass is the most bountiful renewable carbon resource on earth. Photocatalytic transformation is a promising method to utilize biomass to obtain high-value-added chemicals and it has more obvious advantages compared with thermochemical and biological processes due to the milder operational conditions, fewer reagents and equipment. Semiconductor material is one of the most common kinds of heterogeneous biomass photocatalysts, which has the advantages of high selectivity, stable catalytic performance, long activation time, and low cost. In this paper, the significant research progress on the photocatalytic transformation of biomass with semiconductor materials to produce high-value-added chemicals is reviewed, and the three most typical semiconductor photocatalysts (TiO_2, CdS, and g-C_3N_4) are detailed. The photocatalytic mechanism and photocatalytic system optimization including structural modification, metal co-catalyst loading, and introduction of heterojunction are presented. Besides, the main problems, the development direction and trend of semiconductor materials in photocatalytic transformations of biomass in the future are prospected, which provide guidance and inspiration for the further development of semiconductor photocatalysts and make contributions to the progress in efficient utilization of biomass.

1. Introduction

With the swift growth of the economy, the total demand for energy in the world is skyrocketing year by year. Fossil resources satisfy the majority of the world's energy consumption. However, the use of massive fossil energy has also exacerbated global warming and caused frequent haze. To meet the growing energy needs and alleviate the environmental problems, it is urgent to find a green, abundant, and economic alternative. Biomass is the largest renewable carbon resource, which is considered a promising alternative. It is a highly functionalized feedstock with an organic carbon structure, which is suitable to produce fine chemicals [1,2]. Various processes such as thermochemical and biological transformation have been proposed to convert biomass to high-value-added chemicals.

Nevertheless, for thermochemical transformation, harsh reaction conditions (such as high pressure or high temperature) and enormous energy consumption are inevitable [3–5]. In addition, it is hard to accurately transfer energy to the target reactants or chemical bonds, generating a low energy utilization rate.

Moreover, biomass usually has multiple functional groups, so selectively activating a specific functional group is out of the question, causing the low selectivity of the target product with various by-products [6–8]. As for biological transformation, the obstacle that must be overcome is the huge investment including costly reagents and equipment [9,10]. As an emerging technology, photocatalysis has attracted increasing concerns thanks to its harmlessness, environmental protection, sustainability, mild operational conditions, and cheapness [11,12]. Photocatalysis is a process in which inexhaustible solar energy can be converted into chemical energy and trigger the transformation of material (such as biomass) under the irradiation of light [13,14]. When biomass is the substrate of photocatalytic reaction, a variety of key fine chemicals, such as 2,5-dicarbonyl furan (DFF) [15] and 5-hydroxymethylfurfural (HMF) [16] can be obtained. Further, H_2 can also be got if an appropriate amount of electron donors is added [17].

The development and design of high-efficiency photocatalysts, the key to photocatalytic reaction, are a critical part of the photocatalytic transformation of biomass. There are two types of photocatalysts, homogeneous and heterogeneous photocatalysts [18–20]. The latter has better practical potential as it is more inexpensive and easier to separate [21–23]. The semiconductor mate-

* Corresponding author.
E-mail address: wjq@xjtu.edu.cn (J. Wang).

https://doi.org/10.1016/j.cclet.2023.108723
1001-8417/

rial is a kind of the most common heterogeneous biomass photocatalyst due to its high selectivity, stable catalytic performance, long activation time, and low cost, with the most perfect examples being TiO_2, CdS, and g-C_3N_4 [24]. To the best of our knowledge, some excellent reviews have appeared in the literature. Wu *et al.* [25] provide a critical review of photocatalytic transformations of bio-based platform compounds to high-value chemicals. Alberto V. Puga [26] summarized a specific overview of biomass-to-H_2 routes. Considering the prospect of semiconductor material in the field of photocatalysis research, a comprehensive summarization of semiconductor photocatalytic mechanism and modification methods is needed to clarify the emerging research field of solar energy-driven biomass conversion.

This review mainly introduces the semiconductor materials represented by TiO_2, CdS, and g-C_3N_4 in the photocatalytic transformation of biomass, details the photocatalytic mechanism and the ways to promote the photocatalytic efficiency, such as structural modification, metal co-catalyst loading, and introduction of heterojunction. The existing problems, future development direction, and trend toward biomass photocatalysis prospects are in the last section.

2. Different semiconductors on biomass photocatalytic transformation

The semiconductor has a unique energy band structure, which consists of a low-energy valence band (VB) and a high-energy conduction band (CB). And the band gap between CB and VB is called the forbidden band, *i.e.*, energy gap (E_g). In a typical photocatalytic process (Fig. 1a), the semiconductor absorbs light energy and generates high-energy electron (e^-) and hole (h^+) pairs, and chemical reactions are activated by detached charge carriers. Importantly, the capacity of the photogenerated carriers (e^--h^+ pairs) to facilitate a redox reaction depends on the potential of VB and CB.

Biomass photocatalytic transformation in general involves the hydrogen evolution reaction (HER) and biomass oxidation reaction (BOR). These two steps may be realized concurrently in one step by the photogenerated electrons and holes over semiconductor photocatalysts. The HER typically occurs over the photocatalyst with CB electrons to reduce protons (H^+) and generate H_2. In contrast, the biomass oxidation reaction is complex and strongly depends on the substrate, catalyst surface, and reaction conditions. The holes with high oxidation potential are commonly considered the major active species responsible for biomass oxidation. In this process, the biomass is moved to a different potential energy surface and resulting in the evolution from the reactant to the product state (Fig. 1b). Essentially, the energy of the charge carrier is converted into the vibrational energy of the activated chemical bond [27].

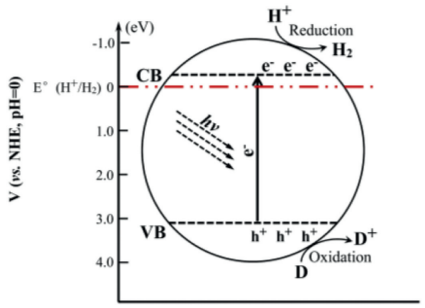

Fig. 2. Basic principle of photocatalysis on TiO_2.

More generally, photocatalytic transformations of biomass are mostly carried out under mild conditions. Through a well-designed semiconductor material, photon-generated carriers can carry out selective cleavage or functionalization of the targeted chemical bond. Thus, photocatalysis has greater potential to accomplish the selective conversion of biomass compared to conventional transformations.

2.1. TiO_2-based material

TiO_2 was the first example used to investigate the photocatalytic reforming of carbohydrates in 1980 [28]. It was found that the conversion of cellulose under light irradiation (500 W Xe lamp) produced H_2 with a quantum yield of 0.3%. Fig. 2 showed the photocatalytic mechanism of TiO_2. It can be summarized that CB is lower than normal hydrogen electrode (NHE) and VB is higher than biomass oxidation. Low CB is favorable for photo-generated electron hydrogenolysis [29], and high VB could efficiently drive the fission of C–C and C–O bonds. Meanwhile, the band gap of TiO_2 (3.0∼3.3 eV) is less than 3.4 eV, which can maintain the stable catalytic effect under the irradiation of ultraviolet (UV) (<387 nm) [30]. Generally, raw TiO_2 exhibits lower efficiency in biomass photocatalysis, because of the rapid electron-hole recombination, which limits its industrial application [31]. Time-resolved spectroscopic showed that the diffusion of electrons from the semiconductor to the active site occurs on a timescale of picosecond to nanoseconds [32]. Thus, 90% of electrons and holes would recombine after excitation, which often results in a lower quantum yield. These drawbacks can not be overcome by only optimizing the material itself. Various other strategies to cope with these problems have also been developed [33]. In the following part of this section, the method of modifying the catalyst structure of TiO_2 to improve the target yield will be discussed from the following three aspects: (1) Loading of metal elements, (2) construction of heterojunction, and (3) selection of catalyst carrier.

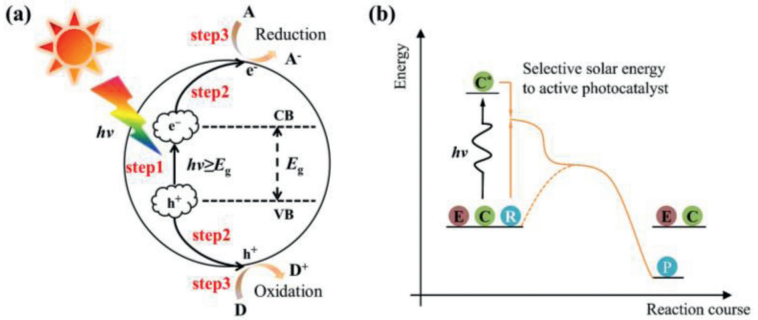

Fig. 1. (a) Photocatalysis principle of semiconductor materials and (b) energy diagram of photocatalysis for the transformation of reactant (R) to product (P). C and E refer to the catalyst, and molecules in the environment, such as solvent and atmosphere.

2.1.1. Loading of metal elements

Metal species play a special part in photocatalytic reactions. In detail, the metals act as active sites for H_2 production on the surface of TiO_2 [34]. Generally, Pt is one of the most effective and investigated co-catalyst due to its low overpotential of NHE and large work function. [35]. Bellardita *et al.* [36] examined the conversion of glucose to arabinose with Pt-TiO_2 under photocatalysis. Results showed that the conversion yield of glucose under 700 W medium pressure Hg lamp was 92%, about 7.6 times higher than the raw TiO_2 (12%). Authors found that Pt was uniformly scattered on the surface or matrix of TiO_2 particles in the shape of clusters or mononuclear complexes. About 0.5 electrons per Pt atom transferred from the d-orbital to the s-orbital in the reaction, thus, the 5d-orbital would have an excess of vacant orbitals, which can better capture photo-generated electrons and inhibit electron/hole recombination [37].

To further improve the conversion yield of the substrate, researchers have studied the effect of multi-metal co-loading in TiO_2. Bi/Pt-TiO_2 was used to convert lignin to valuable compounds in the photocatalytic process [38]. Results indicated that Pt provided active sites to alleviate the problem of photo-generated e^--h^+ pairs recombination. In this system, Bi served as a promoter to boost the generation of $O_2^{\bullet-}$ from trapped photo-electrons. The conversion yield of lignin reached 84.5% after 1 h irradiation, while in the Pt-TiO_2 system, the conversion rate of lignin was only 28.23%. This research provides a novel opportunity for the transformation of biomass using Bi and noble metal-based co-catalysts under solar radiation.

Asides from Pt, Ag is another common co-catalyst of TiO_2 in the photocatalytic process. However, the catalytic effect mechanism of Ag is quite different from Pt, which is affected by the dispersion model and electronic properties [39]. The better photocatalytic effect of Ag-TiO_2 is owing to the difference in the Fermi energy of TiO_2 and Ag [40]. Higher Fermi energy in Ag can form a Schottky barrier, which contributes to the electron-hole pair separation. Xu *et al.* [41] also studied the synergistic effect of interfacial lattice Ag^+ and Ag^0 clusters in enhancing the photocatalytic. Results showed that photo-generated electrons can transfer CB (TiO_2) to the Ag^0 cluster quickly and smoothly, resulting in improving the photocatalytic activity of $Ag^+/TiO_2@Ag^0$.

Besides Pt and Ag, some typical metals, like Au [42], Pd [43], Bi [44] and Ni [45], also can improve photocatalytic activity by building numerous oxidation reaction active sites (Table 1). The choice of loading metal to TiO_2 is vital to photocatalytic efficiency. The metals have a low overpotential for H_2, which can make it easier to generate H_2 [46,47]. When TiO_2 is loaded with these metals, the electrons migrate from TiO_2 to the noble metal. Thus, the metals can serve as active sites for H_2 production on the TiO_2 surface. To sum it up, the lower the overpotential of the metal, the higher the activity it shows. However, metal loading amount is also another key parameter that affects the photocatalytic reaction. Deposited metal can promote photo-generated carrier separation effectively, whereas excessive metal loading reduces photocatalytic efficiency [48,49]. Specifically, superfluous metal particles form metal clusters or blocks on the surface of the semiconductor, impeding light absorption. In addition, in most studies, the reusability and stability of catalysts were not detail discussed due to the well-known stability of TiO_2 [50].

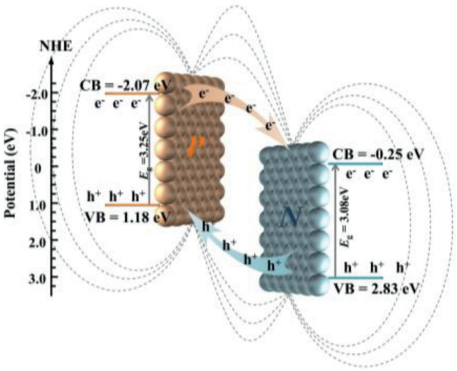

Fig. 3. Photocatalytic mechanism of TiO_2-NiO n-p heterojunction under simulated light irradiation. Reproduced with permission [53]. Copyright 2020, Elsevier Inc.

2.1.2. Construction of heterojunction

Constructing heterojunction is an effective way to regulate the band gap of TiO_2 in photocatalytic transformation [51,52]. TiO_2 is a typical n-type semiconductor (electron-rich), which can combine with a p-type semiconductor (hole-rich) to form a typical staggered gap structure (n-p junction). Two semiconductors possess different band gap structures, and they can form the built-in electric field due to the spontaneous diffusion of electrons. The photo-generated electrons under suitable irradiation could be forced to move through the built-in electric field, therefore inhibiting the recombination of e^--h^+.

NiO is a common p-type semiconductor. It can construct an n-p heterojunction with TiO_2 on account of staggered band structures. Zhao *et al.* [53] prepared TiO_2-NiO through a one-step hydrothermal method. TiO_2 nanoparticles were coated by NiO nanoclusters and results showed that TiO_2-NiO had high reaction activity (Fig. 3). The apparent quantum yield (AQY) of TiO_2-NiO reached

Table 1
Influence of TiO_2 photocatalyst structure on photocatalytic transformation performance.

Photocatalyst	Co-catalyst	Biomass derivatives	Light source	Products	Catalytic efficiency		Reusability	Stability	Refs.
TiO_2(US)	–	Glucose	125 W (Hg)	Glucaric acid, gluconic acid, and arabitol	Glucose conversion	11%	/	/	[46]
TiO_2(P25)	–	Glucose	125 W (Hg)	Formic acid	Glucose conversion	79.6%	Four cycles	/	[47]
TiO_2	0.5 wt% Pt	Cellulose (CLS)	UV-A	H_2	H_2 evolution efficiency	54 μmol (4 h)	/	/	[48]
TiO_2	1 wt% Pt 0.5 wt% Pd 1 wt% Pd 1 wt% Au	Glycerol	UV ($\lambda = 365$ nm)	H_2	Rate of H_2 production (mmol g^{-1} h^{-1})	27.1 41.1 47.5 29.8	/	/	[43]
TiO_2	0.5 wt% Pt	Sub-micron sized cellulose particles	UV - visible light (iron-halide lamp)	H_2 and HCOOH	Products yield	81.2%	Two cycles	Two cycles	[46]
TiO_2(R)	0.2 wt% Rh	Glucose	300 W (Xe)	Arabinose, Erythrose, and H_2	The amounts of the products	445 μmol (4 h)	/	/	[49]

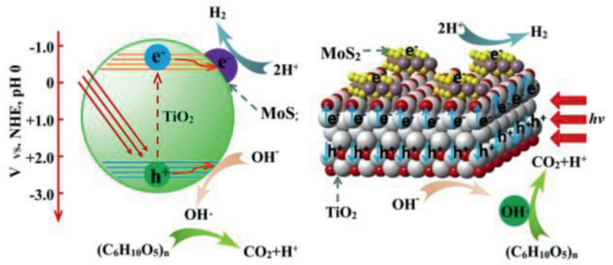

Fig. 4. Energy diagram of charge transfer and proposed reaction mechanism for photocatalytic H_2 production from lignocellulose over 2D-2D MoS_2/TiO_2 photocatalysts. Copied with permission [54]. Copyright 2021, Wiley-VCH GmbH.

6.46% under 365 nm monochromatic light, which was around 2.9 times greater than that of raw TiO_2. Besides the core-shell structure of the n-p junction, Wang *et al.* [54] reported a large 2D nano junction photocatalyst by growing 2D MoS_2 nanosheets on the superficial of TiO_2 (Fig. 4). 2D-2D MoS_2-TiO_2 photocatalysts were constructed to convert lignocellulose to H_2. An AQY of 1.45% (H_2) was acquired under 380 nm (Xe) over MoS_2(2%)-TiO_2, which is better than the current TiO_2-based photocatalysts.

The construction of heterojunctions has been demonstrated as one of the most efficient methods to upgrade the spatial separation of carriers. However, in the process of synthesizing heterojunction, some defects at the interface or surface states would be formed, which is harmful to the form of the built-in electric field. Therefore, a simple and steady synthetic method is very necessary to gain impeccable nanocomposite architecture.

2.1.3. Selection of catalyst carrier

Pure nanoscale TiO_2 has the disadvantage of being easily aggregated in solution, which decreases the specific surface area of the catalyst. A better carrier should not only provide a rich reaction site and large surface area but also promote the reaction through its physical and chemical properties [55]. The most common catalyst carrier is acidic zeolite. Wang *et al.* [56] combined TiO_2, Au, and zeolite HY to form Au-HYT. Au-HYT was used to convert cellulose to glucose with a yield of 48% under light irradiation at 140 °C. Zeolite HY plays a pre-decomposition role in cellulose, which makes the reaction easier. As the reaction continues, HMF was also produced as a co-product, and the overall yield of glucose and HMF reached 60%.

Carbon nanotubes (CNT) are another common catalyst carrier. Photo-generated electrons can transfer from TiO_2 to CNTs, thus retards the recombination of photo-generated e^--h^+. Li *et al.* [57] prepared CNT-TiO_2 by sol-gel technique, and the structure of TiO_2-CNTs nanocomposites was shown in Fig. 5. Results revealed that the conversion of CNT-TiO_2 was about two times as high as the conversion of pure TiO_2. Moreover, Takenaka *et al.* [58] loaded Pt on TiO_2-CNT to boost photocatalytic efficiency. When the loading amount of Pt was 1.5%, the photocatalytic activity of TiO_2-CNT@Pt was about 1.6 times over that of TiO_2-CNT and 2.9 times over that of pure TiO_2. As shown in Fig. 6, part of Pt was deposited in the cavity of CNT and the rest was on the outer surface of CNTs. Pt on the outer surface provided a catalytic active center, in addition, the deposited Pt in the cavity would inhibit the reverse reaction.

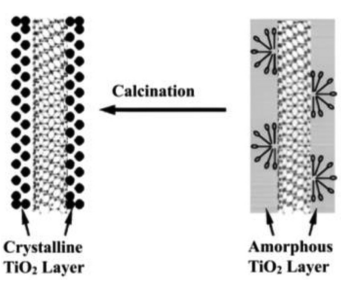

Fig. 5. Structural representation of TiO_2-CNTs nanocomposites. Reproduced with permission [57]. Copyright 2011, Elsevier B.V.

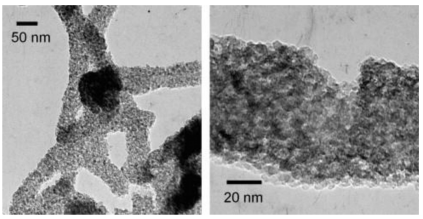

Fig. 6. Transmission electron microscopy (TEM, JEOL-2000EX) images of TiO_2-CNT@Pt. Copied with permission [58]. Copyright 2012, Elsevier B.V.

Generally, the oxidative potential of the photogenerated holes in TiO_2 is around 3.2 eV, which can be viewed as strong oxidants. Nevertheless, this is also the bottleneck of TiO_2, these photo-induced oxidants can oxidize reactant to the final product in one step, thus the selectivity is typically not high. There is still often a trade-off between product selectivity and conversion.

2.2. CdS-based materials

Although the research regarding TiO_2 photocatalytic biomass has obtained a huge development, the inherent shortcomings of TiO_2 photocatalyst like limited light absorption (<387 nm) and serious recombination of photo-generated carriers, still urge scientist to find more types of photocatalyst, and CdS is among these. CdS is a typical II-VI semiconductor photocatalyst, and it has become one of the most potential biomass photocatalyst materials given the advantages of special band structure, diverse modifiability, low price, and simple preparation method [59,60]. At 300 K, the band gap of CdS is 2.4 eV, which allows it to absorb solar energy in a wider spectrum and promote the utilization of light energy (wavelengths shorter than 516 nm). Moreover, comparing the edge position of CB in photocatalyst, CdS is more negative than others (such as TiO_2, $SrTiO_2$, and ZnO), which makes the electrons generated in CdS photocatalytic reaction have a stronger reduction ability.

Research also discovered that the microstructure of CdS had a major effect on photocatalytic activity. Song *et al.* [61] probed into the key role of the microstructure of CdS in the photocatalytic production of amino acids from biomass-based feedstocks. Results showed that the ultra-thin CdS nanosheets had higher activity for lactic acid to produce alanine compared with other forms of CdS (such as nanospheres and nanorods). Moreover, CdS quantum dots (QDs, <6.5 nm) acted greater activity than CdS nanoparticles (20~40 nm) due to the more surface sites and the improved redox ability [25].

Similar to pure TiO_2, pure CdS does not have better photocatalytic efficiency. During the last decades, extensive efforts have been made to enhance the photocatalytic activity and stability of CdS semiconductors. Thus, some important and representative strategies, including loading of co-catalyst, functionalized with ligands, and avoiding photo-corrosion are discussed in the following sections.

2.2.1. Loading of co-catalyst

To better realize the oxidation of biomass and the generation of H_2, the co-catalyst can be loaded on CdS [62]. Loading a co-catalyst on the surface of photocatalysts is a favor for capturing photo-generated electrons or holes so that they can be transferred

Table 2
Influence of co-catalyst on the catalytic efficiency of CdS.

Photocatalyst	Biomass derivatives	Light source	Main products	Catalytic efficiency		Reusability	Stability	Refs.
Ni-CdS	Furfural alcohol	Blue LED (450 nm, 8 W)	H_2	Conversion of furfural alcohol	58.82%	Four cycles	XRD and SEM (Figs. S1-S4)	[63]
NiS-CdS	Lignin	Visible light irradiation ($\lambda \geq 400$ nm)	H_2	H_2 evolution efficiency ($\mu mol\ g^{-1}\ h^{-1}$)	1512.4	Five cycles	XRD, XPS, and metal leaching (Figs. S5-S8)	[64]
				AQE	44.9%			
MoS_2-CdS	Furfural alcohol	300 W Xe lamp	H_2	H_2 evolution activity ($\mu mol\ g^{-1}\ h^{-1}$)	27.16	Four cycles	SEM (Figs. S9-S11)	[65]
Pt-CdS	Porous regenerated cellulose	250 W Xe lamp ($\lambda \geq 420$ nm)	H_2	H_2 evolution efficiency	6.721 mmol/g (5 h)	Three cycles	Metal leaching (Fig. S12)	[66]

to the catalyst surface quickly. Han *et al.* [63] reported a photocatalyst of ultrathin CdS nanosheets loaded Ni as a co-catalyst (Ni-CdS), which can selectively oxidize the biomass-derived alcohol under visible light and obtain H_2 in the meantime. In this nanoarchitecture, the delivery of photogenerated electrons from the CdS to the metal surface, promotes the separation of electron and hole carriers, thereby leading to the performance improvement of photocatalytic H_2 evolution. In this research, the photocatalyst showed excellent catalytic activity and stability. The corresponding products (aldehyde or acid) can be selectively obtained through adjusting the catalyst and reaction conditions. Besides Ni, other co-catalyst, such as NiS [64], MoS_2 [65], and Pt [66] were also used to improve the photocatalyst efficiency (Table 2). Metallic particles deposited on the surface of the semiconductor often serve as collectors for photo-generated electrons and catalyze the reduction of protons to H_2, depending on the work function of the metal and the potential of the redox processes involved.

2.2.2. Functionalized with ligands

Wu *et al.* [67] applied CdS QDs to the photocatalysis of lignin and realized efficient conversion of native lignin and full utilization of lignocellulose under visible light and mild conditions for the first time. CdS QDs highly dispersed in the solvent can contact native lignin well during the reaction process, so they present excellent catalytic performance. The cleavage of the β-O-4 bond in lignin is achieved by an electron-hole coupled photoredox mechanism on account of Cα radical intermediate, where both photogenerated e^--h^+ take part in the reaction (Fig. 7a). For further confirmation of the role of organic ligands stuck to CdS QDs in the photocatalysis of lignin, Wu *et al.* [68] systematically researched the photocatalytic conversion of native lignin by employing CdS QDs with various surface ligands (Fig. 7b). Photocatalytic behavior of CdS QDs is strongly linked to the organic ligands structure in the transformation from raw lignin to high-value functionalized aromatics.

The hydrophilicity/hydrophobicity of ligands is vital for the joint connection between QDs and lignin, bringing about the better catalytic activity. Ligands also take part in the key step of the photocatalysis-electron transfer process with the mechanism of ligand-mediated electron tunneling.

The photocatalytic activity of CdS can be also enhanced by surface modification. Zhang *et al.* [69] prepared [SO_4]-CdS catalyst by importing surface sulfate ions on CdS catalyst. The surface sulfate ion [SO_4] can be used as a proton receptor to effectively shorten the distance of proton transmission and promote the transfer of proton-coupled electrons. In the photocatalytic reaction of biomass polyol to synthesis gas, the production rate of CO and H_2 are is 9 times and 3 times than pure CdS, respectively.

We ascribed the high activity of this hybrid photocatalytic system to improvement in charge carrier separation and the efficient electron transfer from the CdS to ligands. On the other hand, the hydrophilic ligands rendered the water-insoluble catalyst well-dispersed in an aqueous solution. The encapsulation of the nanoscale semiconductor particles by ligands prevented the catalyst from aggregating and improved the efficiency of active sites.

2.2.3. Avoiding photo-corrosion

CdS could suffer from serious photo-corrosion and continual recombination of photo-generated e^--h^+ in the photocatalytic process. Photo-corrosion of CdS is attributable to an irreversible oxidation reaction driven by photo-generated holes. Under long-term visible light, CdS will be decomposed ($CdS + 2h^+ = Cd^{2+} + S^{2-}$) and then Cd^{2+} will be dissolved into liquid part [70], which seriously affects the photocatalytic stability. In addition, due to the narrow band gap (2.4 eV) of CdS, the electrons in VB transited to CB will recombine with the holes in a few picoseconds. To upgrade the photocatalytic performance of CdS, it is essential to optimize the contact environment between CdS and the reactant interface, thus promoting the separation and transfer efficiency of photogenerated e^--h^+.

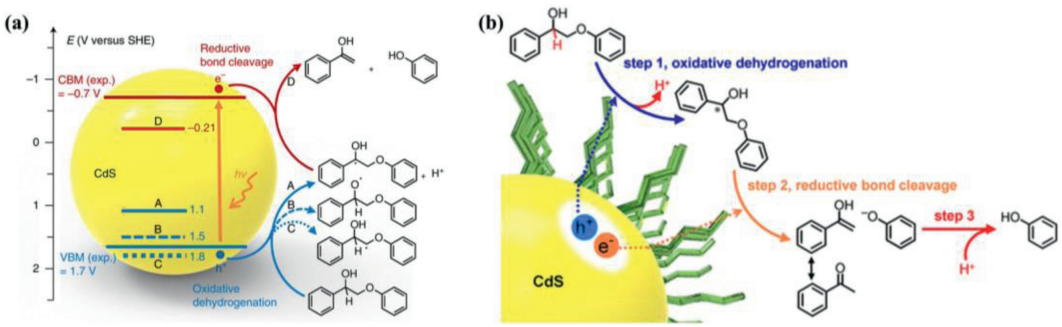

Fig. 7. (a) The potential cleavage of lignin by CdS. Copied with permission [67]. Copyright 2018, Springer Nature Limited. (b) The schematic illustration of the ligand-mediated electron-hole coupled mechanism. Copied with permission [68]. Copyright 2019, American Chemical Society.

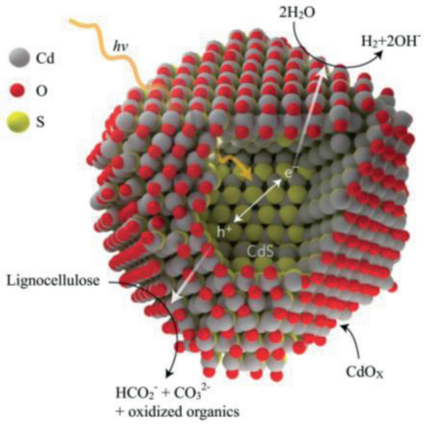

Fig. 8. Photocatalytic transformation of lignocellulose to H_2 on CdS/CdO_x. Copied with permission [71]. Copyright 2017, Nature Publishing Group.

Among synthetic methods aiming at increasing the stability of CdS, the formation of a surface layer on CdS proved beneficial over successive cycles. This strategy forms core/shell structures with protective layers on the surface of CdS nanoparticles, inhibiting corrosion effectively. Wakerley *et al*. [71] constructed a CdO_x protective shell on the outside surface of CdS under alkaline conditions (Fig. 8). The obtained photocatalyst (CdS/CdO_x QDs) can be applied in the oxidation of unprocessed lignocellulosic substrates to achieve the light-driven H_2 evolution without photo-corrosion. Meanwhile, the quantum dots in CdS/CdO_x provide a place for biomass oxidation reaction and enhance the separation of photogenerated e^--h^+. The system could operate stably under visible light beyond six days and produce high H_2 production rate (1∼9 mmol g^{-1} h^{-1}).

Taking these mechanistic fundamentals into account, an efficient and stable photocatalyst system based on CdS semiconductors should achieve high efficiency in visible-light harvesting, and facilitate the photogenerated charge carrier separation. Despite this progress, some challenges still need to be addressed. Firstly, the current CdS photocatalyst systems are still far from being used for industrial production with both economic and environmental benefits. There are environmental and toxicity concerns about the potentially harmful release of cadmium. Additionally, the photo corrosion of CdS and the poor photostability are still key problems obstructing large-scale applications.

2.3. g-C_3N_4 based materials

Nitrogen-rich organic precursors, such as thiourea, urea, cyanamide, dicyandiamide, as well as melamine, can be used to fabricate g-C_3N_4 by thermal polymerization method [72]. g-C_3N_4 is a distinctive carbon material, which is one of the most steady allotropes of carbon nitrides. g-C_3N_4 is a better photocatalyst due to its mild bandgap energy of 2.7 eV (460 nm) [73] as well as proper CB (−1.1 eV) and VB (+1.6 eV) [74]. In the recent decade, among various semiconductors, g-C_3N_4 is one of the most utilized semiconductors in various photocatalytic processes, due to its numerous advantages like non-toxicity, bio-compatibility, low cost, and high photochemical and thermal stability.

Rao *et al*. [75] peeled monolayer g-C_3N_4 from bulk g-C_3N_4 by nitrogen-protected ball milling method (Fig. 9). The obtained monolayer g-C_3N_4 retains the intrinsic structure with an atomic layer. This structure can degrade the exciton binding energy, cut down the charge transport distance, and stimulate the separation efficiency of carriers. As a result, effectively ameliorative its performance of photocatalytic degradation of lignocellulose. Results

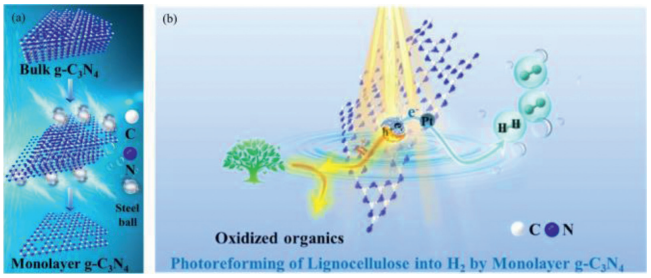

Fig. 9. (a) The physical exfoliation of monolayer g-C_3N_4; (b) H_2 generation through the photocatalytic transformation of lignocellulose with monolayer g-C_3N_4. Copied with permission [75]. Copyright 2021, American Chemical Society.

showed that monolayer had better photocatalyst performance in cellulose (872 μmol $H_2 \cdot g_{cat.}^{-1}$), hemicellulose (719 μmol $H_2 \cdot g_{cat.}^{-1}$), and lignin (249 μmol $H_2 \cdot g_{cat.}^{-1}$) conversion under visible light illumination (300 W) after 12 h.

So far, g-C_3N_4 has harvested extensive attention due to its unique two-dimensional structure [76]. It has also emerged as one of the satisfactory stable organic polymers [77,78]. Many modifications have been proposed to ameliorate the photocatalytic capability of g-C_3N_4 by employing various strategies, such as surface defects (N-defected g-C_3N_x) [79], ultrafine structures [80] and QDs/g-C_3N_4 [81].

2.3.1. Loading of metal elements

Similar to TiO_2 and CdS, the catalyst efficiency of g-C_3N_4 can be tuned by modifying the band structure, for instance, by loading metals in biomass photocatalytic transformation [82]. Yang *et al*. [83] used bimetal (Ni-Au) to modify g-C_3N_4 (Ni-Au/g-C_3N_4) by a step-by-step photo-deposition method, thus promoting the co-production of furfural and H_2 from furfural-alcohol aqueous solution. The product yields with Ni-Au/g-C_3N_4 catalyst were significantly improved and almost 3.2 and 2.9 times higher than bare g-C_3N_4 and Au/CN photocatalyst, respectively. Results showed that g-C_3N_4 was the main light-harvesting substance for generating e^--h^+ pairs. Photo-generate carriers could be separated efficiently at Ag/g-C_3N_4 interface and Ni could be worked as both electron capture and active sites for H_2 evolution.

Nonetheless, g-C_3N_4 has some inherent disadvantages such as inefficient visible-light absorption (below 460 nm), less active sites for interfacial reactions, and inefficient specific surface area (about 10 m^2/g). The design of perfect-activity g-C_3N_4 is highly dependent on the morphology, plentiful reactive sites, and especially extended light-harvesting ability. However, the superior metal-free properties of g-C_3N_4 have not received enough importance, with only a few research focusing on the photocatalytic transformation of selected biomass derivatives.

3. Conclusion and outlook

Semiconductor photocatalysts are always a research hotspot due to their unique energy band structure and excellent photocatalytic performance. Applications of semiconductor materials in photocatalytic reforming of biomass and its derivatives have realized the rational utilization of biomass resources, which is of great emphasis to alleviate the crisis of fossil energy and realize the sustainable development of the environment. Increased requirements for establishing a clean and green energy system, combined with escalating environmental standards and government initiatives, have all contributed to an in-depth study in photocatalysis. Research and development on using semiconductors as efficient catalysts can play a vital role in advancing the practical application of photocatalytic technology. At present, this technology has successfully real-

ized the conversion of a variety of biomass and its derivatives to H_2 and high-value chemicals. In this paper, the influences of TiO_2, CdS, and g-C_3N_4 on valuable products from photocatalytic transformation biomass were discussed thoroughly with representative instances.

Section 2.1 (TiO_2-based materials) focuses on discussing the effects of the conversion of biomass by photocatalytic transformation. Despite many methods that have been realized to enhance its photocatalytic activity, like metal particle loading and constructing heterojunction, industrialization is yet to be realized. For CdS-based materials part (Section 2.2), the influences of photocorrosion, co-catalysts, and surface ligands on biomass conversion under photocatalytic transformation were summarized. For M-CdS, in many works, it gave desirable photocatalytic transformation activity, but its environmental toxicity remains yet to be worked out. A brief introduction to g-C_3N_4 based material was shown in Section 2.3. Due to its structural and semiconductor optical properties, g-C_3N_4 has shown great potential as a catalyst in energy conversion.

Based on the existent research progress on biomass conversion under photocatalytic reaction, we propose the following views and opinions:

(1) The modification of photocatalyst. As we have seen, the efficiency of photocatalytic transformation of selected biomass derivatives is still low for most semiconductor photocatalysts. The commonly used evaluation parameters are the conversion of biomass, the rate of H_2 generation as well as quantum yield. However, part of the incident sunlight energy can be stored in the final H_2 fuel and value added chemicals. In this regard, the energy efficiency of the overall sum of processes, starting from raw biomass and concluding with H_2, is a parameter of paramount importance. Up to now, there is still a great deficiency between the present studies and industrial expectations in biomass conversion. An ideal photocatalyst is needed to perform the reaction mildly with high efficiency. Photocatalyst development is a major bottleneck for the semiconductor photocatalysis of biomass to obtain valuable products.

(2) The exploration of mechanism. In current studies, the photocatalytic process of semiconductor materials has been clearly defined, but the fracture and formation paths of chemical bonds in the biomass photocatalytic reaction are vague. Most studies only reveal the relationship between material structures and experimental results, and a few articles cover the catalytic mechanism but still do not explain it thoroughly. The development of isotope labeling may help us in further understanding. Further clarification of the catalytic mechanism will greatly heighten the application performance of semiconductors and expand the broader application areas.

(3) The selection of substrate. Most studies chose to use pure substances to explore photocatalytic performance. Biomass is very complex and recalcitrant with various functional groups, which have abundant C–O and C–C bonds. Its composition and proportion vary from source to source, and the mechanism of interaction between components is complex. Expanding the range of substrates and making efficient use of biomass are the directions of further research.

(4) Cost-benefit analysis. There is no doubt that the photocatalytic transformation of selected biomass derivatives helps to take advantage of solar energy. However, before industrialization, the cost-benefit analysis should ensure it conforms to economic feasibility. The reusability and stability of catalysts are crucial factors to reduce the cost of industrialization. In addition, related analysis shows that further engineering of the photoreactor is crucial to improve light penetration and mass transfer for optimal photon absorption. Thus, from an economic standpoint, apart from photocatalyst design, photoreactor engineering should be given equal consideration in future investigations.

Declaration of competing interest

The authors declare that they have no known competing financial interests or personal relationships that could have appeared to influence the work reported in this paper.

Acknowledgments

The authors are grateful for the financial supports provided by the National Natural Science Foundation of China (Nos. 22108221 and 52203145) and the Shaanxi Natural Science Foundation (No. 2021JQ-028). The authors wish to thank Yayun Ma (Core Facilities and Experiment Center of Xi'an Jiaotong University) for technological guidance.

Supplementary materials

Supplementary material associated with this article can be found, in the online version, at doi:10.1016/j.cclet.2023.108723.

References

[1] Y.M. Bar-On, R. Phillips, R. Milo, Proc. Natl. Acad. Sci. U. S. A. 115 (2018) 6506–6511.
[2] R. Kumar, V. Strezov, H. Weldekidan, et al., Renew. Sustain. Energy Rev. 123 (2020) 109763.
[3] S.P. Guo, Q.B. Liu, J. Sun, et al., Renew. Sustain. Energy Rev. 91 (2018) 1121–1147.
[4] S.K. Bhatia, A.K. Palai, A. Kumar, et al., Bioresour. Technol. 340 (2021) 125644.
[5] H.W. Lee, H. Lee, Y.M. Kim, et al., Chin. Chem. Lett. 30 (2019) 2147–2150.
[6] Y. Li, B. Xing, Y. Ding, et al., Bioresour. Technol. 312 (2020) 123614.
[7] T.Y.A. Fahmy, Y. Fahmy, F. Mobarak, et al., Environ. Dev. Sustain. 22 (2020) 17–32.
[8] T. Kan, V. Strezov, T.J. Evans, Renew. Sustain. Energy Rev. 57 (2016) 1126–1140.
[9] X. Hu, M. Gholizadeh, J. Energy Chem. 39 (2019) 109–143.
[10] A.T. Hoang, H.C. Ong, I.M.R. Fattah, et al., Fuel Process. Technol. 223 (2021) 106997.
[11] W.S. Koe, J.W. Lee, W.C. Chong, et al., Environ. Sci. Pollut. Res. 27 (2020) 2522–2565.
[12] F. Zhang, X. Wang, H. Liu, et al., Appl. Sci. 9 (2019) 2489.
[13] C.Y. Toe, C. Tsounis, J. Zhang, et al., Energy Environ. Sci. 14 (2021) 1140–1175.
[14] M.Y. Qi, M. Conte, M. Anpo, et al., Chem. Rev. 121 (2021) 13051–13085.
[15] P. Gallezot, Chem. Soc. Rev. 41 (2012) 1538–1558.
[16] U. Nwosu, A. Wang, B. Palma, et al., Renew. Sustain. Energy Rev. 148 (2021) 111266.
[17] K.A. Davis, S. Yoo, E.W. Shuler, et al., Nano Converg. 8 (2021) 6.
[18] H. Liu, M. Cheng, Y. Liu, et al., Energy Environ. Sci. 15 (2022) 3722–3749.
[19] W. Xiao, M. Cheng, Y. Liu, et al., ACS Catal. 13 (2023) 1759–1790.
[20] Q.S. Si, W.Q. Guo, H.Z. Wang, et al., Chin. Chem. Lett. 31 (2020) 2556–2566.
[21] J.C. Colmenares, R. Luque, Chem. Soc. Rev. 43 (2014) 765–778.
[22] Q. Li, X. Li, S. Wageh, et al., Adv. Energy Mater. 5 (2015) 1500010.
[23] Y. Qu, X. Duan, Chem. Soc. Rev. 42 (2013) 2568–2580.
[24] C. Karthikeyan, P. Arunachalam, K. Ramachandran, et al., J. Alloys Compd. 828 (2020) 154281.
[25] X. Wu, N. Luo, S. Xie, et al., Chem. Soc. Rev. 49 (2020) 6198–6223.
[26] A.V. Puga, Coord. Chem. Rev. 315 (2016) 1–66.
[27] S. Linic, U. Aslam, C. Boerigter, et al., Nat. Mater. 14 (2015) 567–576.
[28] T. Kawai, T. Sakata, Nature 286 (1980) 474–476.
[29] K. Shimura, H. Yoshida, Energy Environ. Sci. 4 (2011) 2467–2481.
[30] L. Jiang, S. Zhou, J. Yang, et al., Adv. Funct. Mater. 32 (2022) 2108977.
[31] J. Chen, F. Qiu, W. Xu, et al., Appl. Catal. A 495 (2015) 131–140.
[32] T. Chen, Z. Feng, G. Wu, et al., J. Phys. Chem. C 111 (2007) 8014.
[33] B. Dong, T. Liu, C. Li, et al., Chin. Chem. Lett. 29 (2018) 671–680.
[34] L.G. Devi, R. Kavitha, Appl. Surf. Sci. 360 (2016) 601–622.
[35] A. Caravaca, W. Jones, C. Hardacre, et al., Proc. Roy. Soc. A 472 (2016) 21.
[36] M. Bellardita, E.I. Garcia-Lopez, G. Marci, et al., Int. J. Hydrog. Energy 41 (2016) 5934–5947.
[37] M. Anpo, M. Takeuchi, J. Catal. 216 (2003) 505–516.
[38] J. Gong, A. Imbault, R. Farnood, Appl. Catal. B 204 (2017) 296–303.
[39] Y.S. Fu, J. Li, J. Li, Nanomater 9 (2019) 359.
[40] H. Chakhtouna, H. Benzeid, N. Zari, et al., Environ. Sci. Pollut. Res. 28 (2021) 44638–44666.

[41] L. Xu, D. Zhang, L. Ming, et al., Phys. Chem. Chem. Phys. 16 (2014) 19358–19364.
[42] B. Zhou, J. Song, Z. Zhang, et al., Green Chem. 19 (2017) 1075–1081.
[43] Z.H.N. Al-Azri, W.T. Chen, A. Chan, et al., J. Catal. 329 (2015) 355–367.
[44] Q. Chen, X. Cheng, H. Long, et al., Chin. Chem. Lett. 31 (2020) 2583–2590.
[45] Y. Wei, J. Xiong, W. Li, et al., Inorg. Chem. Front. 5 (2018) 2709–2717.
[46] J.C. Colmenares, A. Magdziarz, A. Bielejewska, Bioresour. Technol. 102 (2011) 11254–11257.
[47] B. Jin, G. Yao, X. Wang, et al., ACS Sustain. Chem. Eng. 5 (2017) 6377–6381.
[48] A. Speltini, M. Sturini, D. Dondi, et al., Photochem. Photobiol. Sci. 13 (2014) 1410–1419.
[49] R. Chong, J. Li, Y. Ma, et al., J. Catal. 314 (2014) 101–108.
[50] G. Zhang, C. Ni, X. Huang, et al., Chem. Commun. 52 (2016) 1673–1676.
[51] H. Yang, Mater. Res. Bull. 142 (2021) 111406.
[52] H. Wang, L. Zhang, Z. Chen, et al., Chem. Soc. Rev. 43 (2014) 5234–5244.
[53] H. Zhao, C.F. Li, L.Y. Liu, et al., J. Colloid Interface Sci. 585 (2021) 694–704.
[54] P. Wang, Y.J. Yuan, Q.Y. Liu, et al., ChemSusChem 14 (2021) 2860–2865.
[55] B. Feng, H. Wang, D. Wang, et al., Nanoscale 6 (2014) 14371–14379.
[56] L. Wang, Z. Zhang, L. Zhang, et al., RSC Adv. 5 (2015) 85242–85247.
[57] Z. Li, B. Gao, G.Z. Chen, et al., Appl. Catal. B 110 (2011) 50–57.
[58] S. Takenaka, T. Arike, H. Matsune, et al., Appl. Catal. B 125 (2012) 358–366.
[59] L. Cheng, Q. Xiang, Y. Liao, et al., Energy Environ. Sci. 11 (2018) 1362–1391.
[60] Y.J. Yuan, D. Chen, Z.T. Yu, et al., J. Mater. Chem. A 6 (2018) 11606–11630.
[61] S. Song, J. Qu, P. Han, et al., Nat. Commun. 11 (2020) 1–10.
[62] G. Han, T. Yan, W. Zhang, et al., ACS Catal. 9 (2019) 11341–11349.
[63] G. Han, Y.H. Jin, R.A. Burgess, et al., J. Am. Chem. Soc. 139 (2017) 15584–15587.
[64] C. Li, H. Wang, S.B. Naghadeh, et al., Appl. Catal. B 227 (2018) 229–239.
[65] L. Zhao, T. Dong, J. Du, et al., Sol. RRL 5 (2021) 9.
[66] D. Ke, S. Liu, K. Dai, et al., J. Phys. Chem. C 113 (2009) 16021–16026.
[67] X. Wu, X. Fan, S. Xie, et al., Nat. Catal. 1 (2018) 772–780.
[68] X. Wu, S. Xie, C. Liu, et al., ACS Catal. 9 (2019) 8443–8451.
[69] Z. Zhe, W. Min, Z. Hongru, et al., J. Am. Chem. Soc. 143 (2021) 6533–6541.
[70] X. Chen, S. Shen, L. Guo, et al., Chem. Rev. 110 (2010) 6503–6570.
[71] D.W. Wakerley, M.F. Kuehnel, K.L. Orchard, et al., Nat. Energy 2 (2017) 1–9.
[72] X. Wang, K. Maeda, X. Chen, et al., J. Am. Chem. Soc. 131 (2009) 1680–1681.
[73] C. Tang, M. Cheng, C. Lai, et al., Coord. Chem. Rev. 474 (2023) 214846.
[74] Y. Gong, M. Li, Y. Wang, ChemSusChem 8 (2015) 931–946.
[75] C. Rao, M. Xie, S. Liu, et al., ACS Appl. Mater. Interfaces 13 (2021) 44243–44253.
[76] R.S. de Almeida Ribeiro, L.E. Monteiro Ferreira, V. Rossa, et al., ChemSusChem 13 (2020) 3992–4004.
[77] M. Ismael, J. Alloys Compd. 846 (2020) 156446.
[78] S. Asadzadeh-Khaneghah, A. Habibi-Yangjeh, J. Clean. Prod. 276 (2020) 124319.
[79] L. Jiang, J. Yang, X. Yuan, et al., Adv. Colloid Interface Sci. 296 (2021) 102523.
[80] H. Huang, L. Jiang, J. Yang, et al., Renew. Sustain. Energy Rev. 173 (2023) 113110.
[81] Y. Chen, M. Cheng, C. Lai, et al., Small 19 (2023) 2205902.
[82] L. Jiang, J. Yang, S. Zhou, et al., Coord. Chem. Rev. 439 (2021) 213947.
[83] Q. Yang, T. Wang, F. Han, et al., J. Alloys Compd. 897 (2022) 163177.